



# Effects of late diagenesis on primary reservoir quality of a quartz arenite unit: a case study from the lower Cretaceous successions of SW Iran

Amirhossein Enayati-Bidgoli<sup>1</sup> · Elham Saemi<sup>2</sup>

Received: 16 May 2018 / Published online: 21 March 2019  
© The Author(s) 2019

## Abstract

In this study, a sandstone interval of the lower Cretaceous successions in SW Iran is analyzed regarding the effects of late diagenesis on the alteration of primary reservoir quality and pore system. Petrological and geochemical analyses indicate dominant quartz mineralogy (quartz arenite) deposited in distributary channel and mouth bar environments which is embedded in delta front to prodelta argillaceous sediments. Rather than mineralogy and some remaining primary (intergranular) porosity, several late (burial) diagenetic processes including multi-phase carbonate cementation, chlorite cementation, and chemical compaction, affected the reservoir quality. Most of the diagenetic processes had a decreasing effect on the primary reservoir quality. All recognized diagenetic features are related to burial diagenesis of the surrounding open marine shales (clay mineral transformation) and expelled diagenetic fluids.

**Keywords** Siliciclastic reservoir · Late diagenesis · Reservoir quality · Rock type · Lower Cretaceous · SW Iran

## 1 Introduction

Siliciclastic rocks have lower diagenetic sensitivity and heterogeneity in comparison with carbonates (e.g., Ebanks et al. 1992; Slatt and Galloway 1992; Lucia 2007; Ahr 2008; Burrowes et al. 2010). Moreover, reservoir heterogeneity could be related to syn-depositional and/or post-depositional diagenetic processes and features, and varies from pore to intra- and inter-field scales (e.g., Slatt and Galloway 1992; Slatt 2006; Lucia 2007; Ahr 2008; Enayati-Bidgoli and Rahimpour-Bonab 2016). In siliciclastic (reservoir) rocks, diagenetic processes are well studied (e.g., Pettijohn et al. 1987; Morad et al. 2012) but their relationships and development mechanisms can be different and crucial in reservoir characterization. For example, a clean and quartz-rich sandstone (quartz arenite) has a low diagenetic potential and is

basically prone to cementation (quartz and carbonate) and compaction (e.g., Pettijohn et al. 1987; Moore 2001).

In this study, a relatively depositionally homogenous quartz arenite reservoir interval of the Lower Cretaceous strata in SW Iran is analyzed (Fig. 1). High degrees of diagenetic modification and cementation as the main characteristics of this thin unit led to a heterogeneously distributed reservoir and non-reservoir intervals despite its depositional homogeneity and high primary intergranular porosity. The main aspect of this study is evaluating the role of burial diagenesis in the alteration of primary reservoir quality and homogeneity, regarding the very low preliminary diagenetic potential of the studied interval.

## 2 Geological setting and stratigraphy

In the Arabian Plate and Zagros fold-thrust belt (Fig. 1a, b), the Cretaceous successions host a considerable part of the world's total hydrocarbon reserves and numerous oil reserves of the Middle East (Setudehnia 1978; Scott et al. 1993; Alsharhan and Nairn 1993; Hollis 2011). Most of hydrocarbon reserves in this region are hosted by carbonate successions. On the other hand, siliciclastic reserves are of lesser importance, especially in Iran. These include

Edited by Jie Hao

✉ Amirhossein Enayati-Bidgoli  
a.h.enayat@gmail.com

<sup>1</sup> Petroleum Geology Department, Research Institute of Petroleum Industry (RIPI), Tehran 14857-3311, Iran

<sup>2</sup> Islamic Azad University, Shahrood Branch, Shahrood 36199-43189, Iran

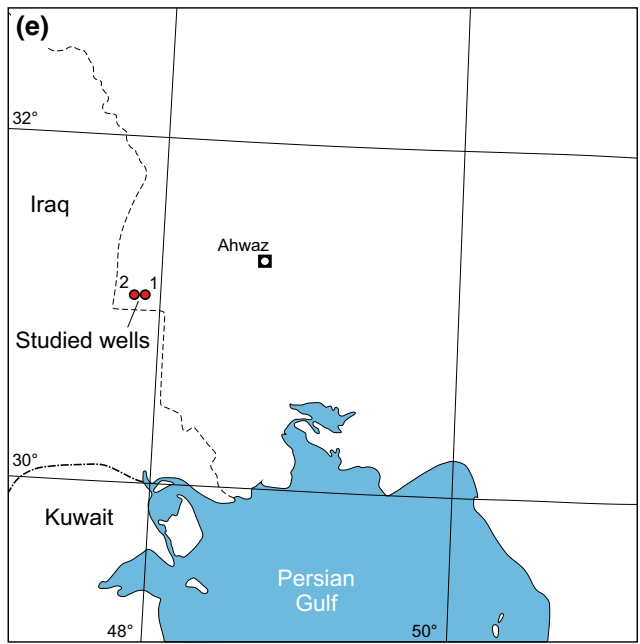
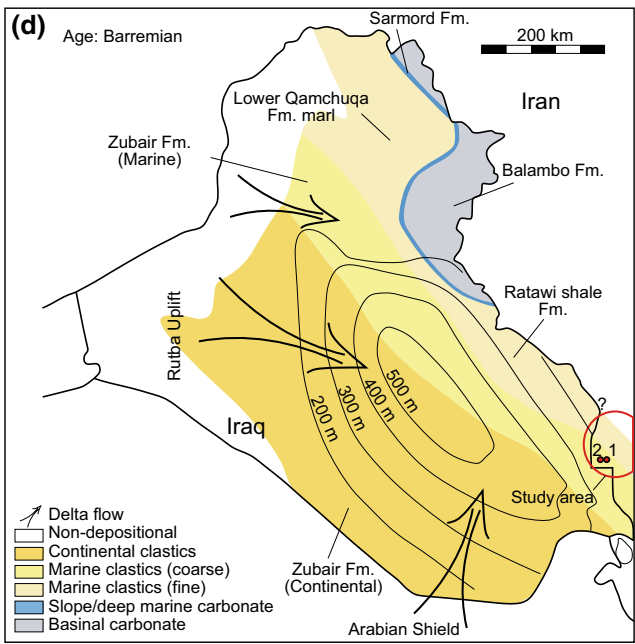
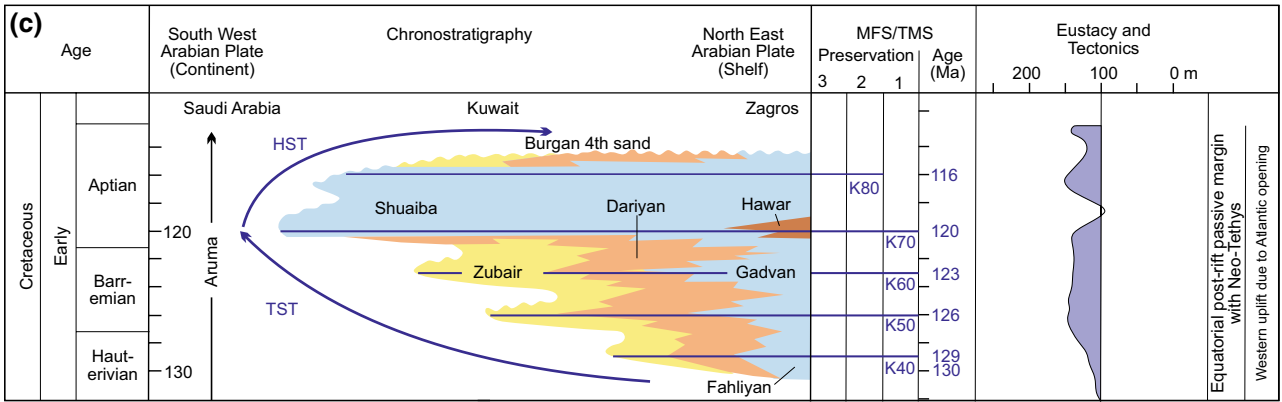
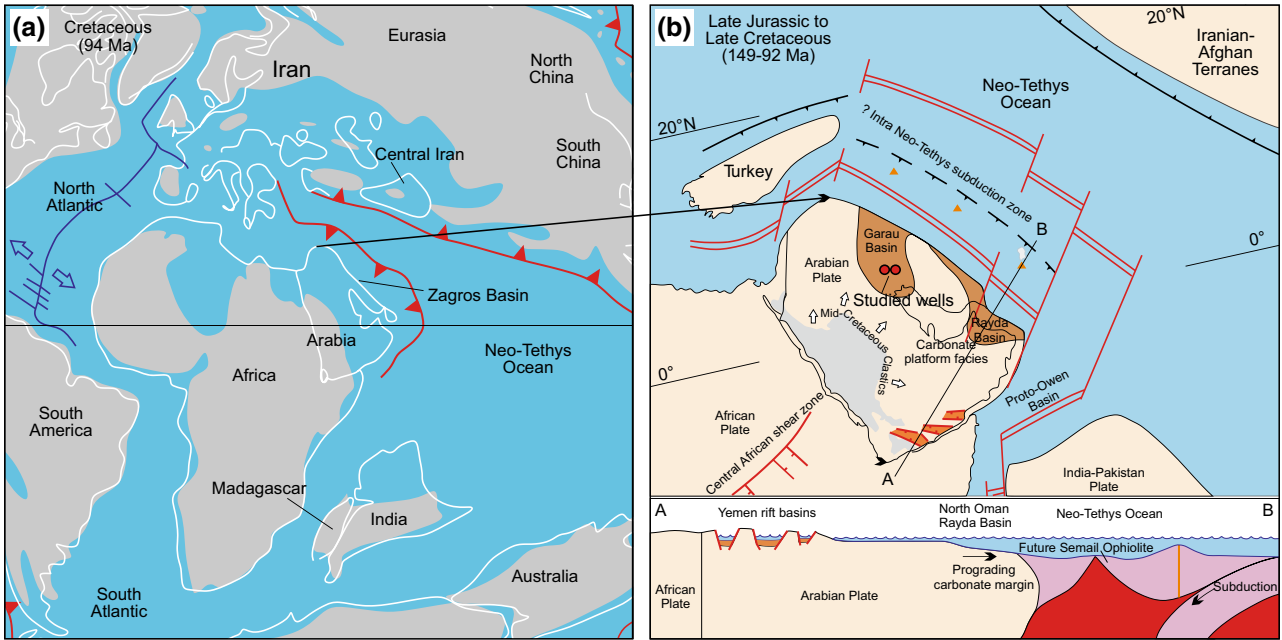


**Fig. 1** a, b Paleogeographic map and plate tectonic position of the Arabian Plate and study area (SW Iran) during the Cretaceous period (modified from <http://paleoportal.org>; Sharland et al. 2001). c Early Cretaceous sequence/stratigraphic diagram of the Arabian Plate and Zagros including main sequence stratigraphic surfaces, lithological changes and formations (modified from Sharland et al. 2001) d Barremian paleogeography and lithostratigraphy of Iraq, Zubair delta and its development directions (arrows) toward Iran, isopach map of the Zubair Formation (lateral equivalent of the Gadvan Formation in SW Iran) and location of the studied wells (Jassim et al. 2006; Aqrabi et al. 2010). e Location map of the studied wells in SW Iran

the Cretaceous Burgan Formation and Azadegan Member. However, they are more frequent in the neighboring Arabian countries (e.g., Sharland et al. 2001; Alsharhan and Nairn 2003; Ghazban 2007).

There are several siliciclastic intervals or reservoirs in the Arabian territories. Toward Iran (Zagros), they are replaced by calcareous—argillaceous successions (Fig. 1c; e.g., Sharland et al. 2001). Throughout the Neocomian—Aptian aged Gadvan Formation (Fig. 1c) encompasses marl or shale, argillaceous limestone, and limestone successions (James and Wynd 1965) with an argillaceous—siliciclastic interval in SW Iran as the lateral equivalent of the lower Zubair Formation of S Iraq (Fig. 1c; e.g., Jassim et al. 2006; Ghazban 2007). The Barremian to Early Aptian aged clastic and deltaic Zubair Formation, as the most prolific reservoir in S Iraq (Fig. 1d; Al-Rawi 1981; Jassim et al. 2006), covers most of the Mesopotamian Basin (Powers et al. 1966; Buday 1980). Toward the Zagros region, it is replaced by the Gadvan marl or shaly limestone (prodelta and open marine depositional settings; Fig. 2; Ali and Nasser 1989; Al-Ameri and Batten 1997; Sadooni and Aqrabi 2000; Bayet-Goll et al. 2016) with several delta-front sand partings (Fig. 2).

During the (Early) Cretaceous, the Arabian Plate was in an equatorial position (Fig. 1a, b; Al-Fares et al. 1998). Due to the central African transtension, the Arabian Plate was uplifted and tilted to the east and provided a sediment source and transport energy to allow the eastward shedding of large volumes of quartz-rich sediments such as the Zubair delta system (Fig. 2a, c; Al-Fares et al. 1998). Such clastic systems (e.g., Ratawi, Zubair, Burgan and Wara) were able to prograde in the face of significant eustatic sea level rise (Fig. 1c; Haq et al. 1988; Sharland et al. 2001). The source of these clastic deltas in central Arabia could be the plutonic igneous rocks of the Arabian Shield (Fig. 1d; Zeigler 2001), but the Zubair sand isolith map in the central and S Iraq suggests influx of clastic sediments from the NW in central Iraq and probably from the SW in S Iraq due to uplift of the Arabian-Nubian Craton (Fig. 1d; Ghazban 2007). They extended to WSW Iran across the border of the Mesopotamian basin and Zagros region, known as the Garau Basin (Fig. 1b). These siliciclastics are composed of monocrystalline and (fluid) inclusion-rich quartz grains and

other detrital fragments such as zircon, rutile and tourmaline (Fig. 3; Table 1; e.g., Folk 1968; Dana 1985; Pettijohn et al. 1987; Gribble and Hall 1995).

The ternary discrimination diagrams for provenance of sandstones (Fig. 4a, b; Dickinson and Suczek 1979; Dickinson 1985) and also paleogeographic maps of the studied area (Fig. 1a, b; Jassim et al. 2006; Aqrabi et al. 2010) indicate a continental interior depositional setting (Fig. 4c; Pettijohn et al. 1987). However, abraded and/or remaining quartz overgrowth cement around the analyzed quartz grains, confirms recycled sandstone (as follows).

### 3 Materials and methods

This study was based on available data from the lower Cretaceous Gadvan Formation in two wells from SW Iran. This included petrophysical well logs (Spectral Gamma Ray, Sonic and Caliper), core, and well cuttings. Moreover, due to the importance of the Gadvan Formation's sandstones, our special focus was on its only sandy part. About 16 whole core samples from the sandy interval of Gadvan with 20 to 30 cm sample spacing were selected for geological and petrophysical (porosity and permeability) investigations and measurements. These were detailed petrographic analysis of prepared thin sections (half stained with Alizarin Red-S and impregnated with blue dyed epoxy resin) and microscopic images of both sandy and shaly intervals of the Gadvan Formation. This led to the identification of petrofacies (PFs), diagenetic processes and products, pore types, and reservoir properties. It must be noted that there were 10 core and 90 cutting samples from the Gadvan Formation's shale.

All depositional and textural properties and also classifications including depositional components by the use of point counting and visual estimation, grain size, roundness, sorting, textural maturity and classification schemes (Wentworth 1922; Folk 1951, 1968; Powers 1953; McBride 1963; Folk et al. 1970; Pettijohn et al. 1987; Jerram 2001) were applied to facies determination. Petrofacies analysis and conceptual depositional model were carried out using standard models, petrofacies descriptions, and the published studies in the neighboring areas (e.g., Pettijohn et al. 1987; Ali and Nasser 1989).

Finally, XRD (bulk and clay), XRF and SEM analyses from sandy and shaly lithologies were available for further and more detailed diagenetic investigations.

### 4 Depositional characteristics

As noted in the geological setting and stratigraphy section, this study is based on the recovered core from the Gadvan Formation or Zubair delta successions. Available

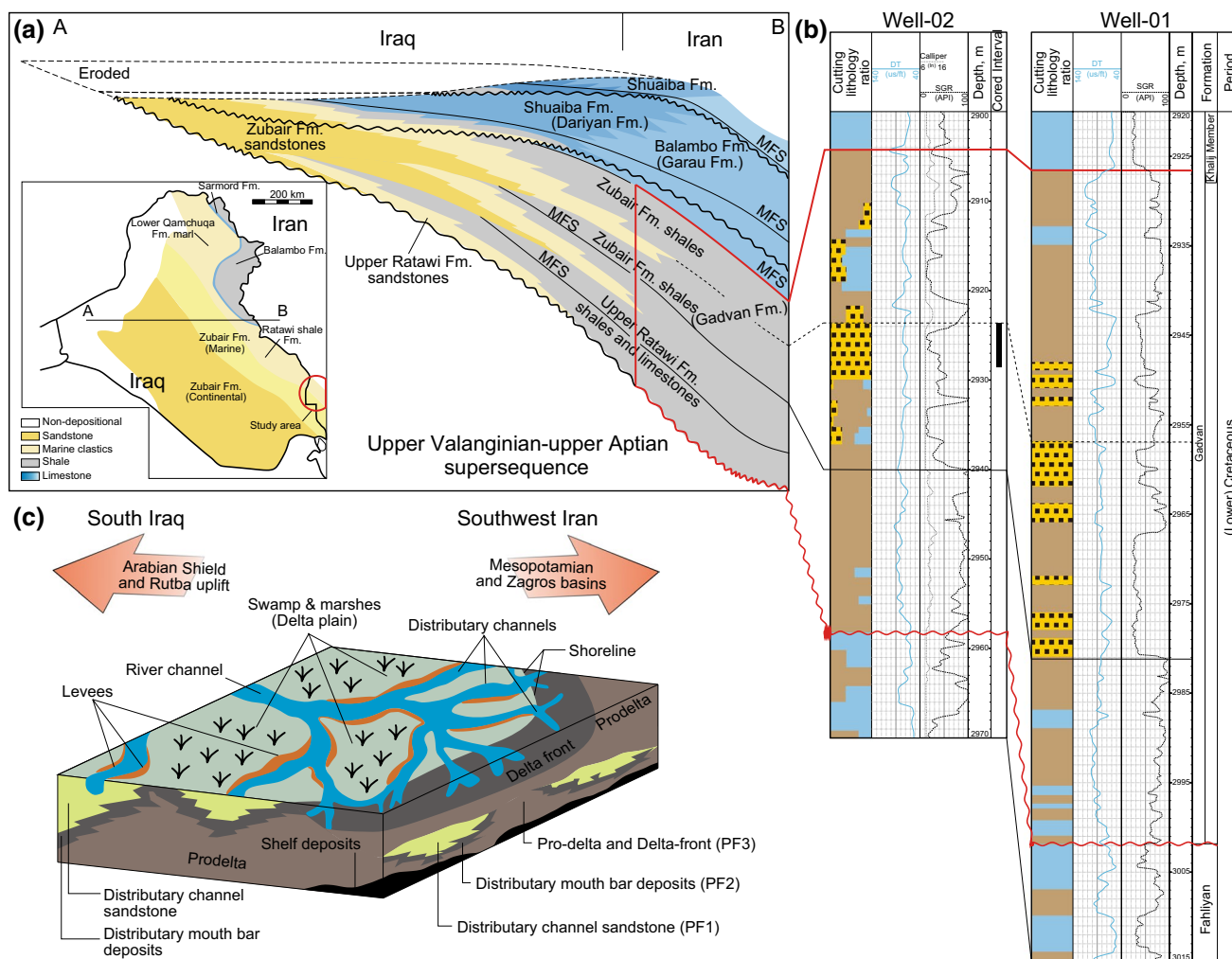


**Fig. 2** **a** The upper Valanginian–upper Aptian supersequence in Iraq toward Iran including the Zubair Formation and its lateral equivalent Gadvan Formation (Aqrawi et al. 2010). **b** Stratigraphic column of the lower Cretaceous studied strata and their equivalents in S Iraq (Aqrawi et al. 2010). **c** A conceptual depositional model of the Lower Cretaceous Zubair Formation in Southern Iraq and its lithostratigraphic equivalent (Gadvan Formation) in SW Iran (Ali and Nasser 1989) along with defined facies in the studied interval

data and references from adjacent areas (Figs. 1d, 3; James and Wynd 1965; Powers et al. 1966; Buday 1980; Al-Rawi 1981; Ali and Nasser 1989; Al-Ameri and Batten 1997; Sadooni and Aqrawi 2000; Ghazban 2007; Jassim et al. 2006; Bayet-Goll et al. 2016) along with well cutting analysis from the un-cored intervals of the studied wells (Fig. 2b) suggest delta front and prodelta depositional settings (Fig. 2c). However, in order to analyze details of the sandy cored interval of the Formation, several parameters including depositional components (Fig. 3), grain size, roundness, sorting, textural maturity and classification schemes (Wentworth 1922; Folk 1951, 1968; Powers 1953; McBride 1963; Folk et al. 1970; Pettijohn et al. 1987; Jerram 2001) were used for facies identification. Based on modal analysis and presented classifications of sandstones and also argillaceous parts, the studied interval is

composed of shale and (quartz arenite) sandstone (Fig. 4c; Table 1), starred numbers refer to samples that selected for more detailed analyses such as XRD, SEM and XRF) and three main petrofacies as follows (Fig. 5):

#### 1. PF1: Well sorted fine quartz arenite

This porous (basically intergranular pores) and oil-stained petrofacies is composed of fine, sub-angular to rounded and well sorted quartz grains which show high textural maturity (super-mature) as a quartz arenite sandstone (Fig. 5a; Table 1). There are rare opaque minerals and feldspars and there are not any visible sedimentary structures at both macroscopic and microscopic scales (Fig. 5b). However, some traces of bioturbation are visible.

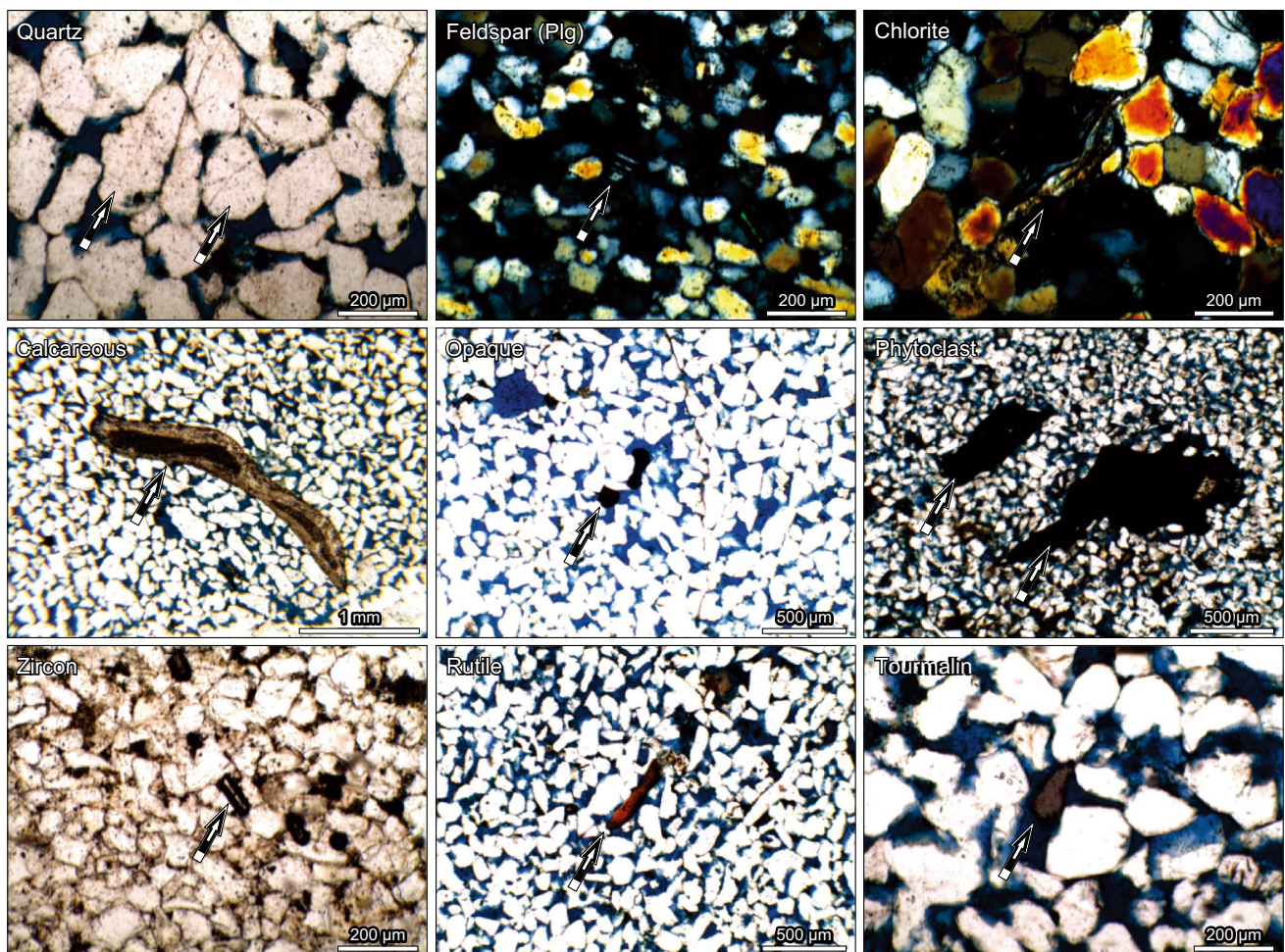


**Fig. 3** All recognized depositional components of the studied sandstone interval

2. PF2: Well sorted very fine quartz arenite

This relatively porous to dense petrofacies is composed of very fine to silt sized, sub-angular to rounded and well sorted quartz grains which show high textural maturity (super-mature) and is a quartz arenite sandstone (Fig. 5c; Table 1). The volume of opaque minerals and to some extent, feldspar is higher than PF1 and also there are thin lamination and bioturbation features at a macroscopic scale (Fig. 5d). The studied samples contain various volumes of carbonate cements (Table 1). The facies frequency diagram (Fig. 2c) shows that the studied sandy interval is mainly composed of PF2.

3. PF3: Shale

Microscopically, this facies is barren and composed of a clayey matrix and dispersed silt sized quartz grains and phytoclasts (Fig. 5e, g). There is some evidence of organic matter among the matrix (Fig. 5e, g). It is visible as fissile and non-fissile shale at core scale (Fig. 5f, h).

According to all available data and evidence, the sandy petrofacies are related to a distributary channel (PF1), and distributary mouth bar (PF2) parts of the Zubair delta which were embedded in delta front and prodelta deposits (Fig. 2c).

## 5 Diagenesis

### 5.1 Diagenetic processes and features

In spite of simple facies (well sorted fine to very fine quartz arenite) and mineralogical content (quartz dominant) of the studied sandstone (quartz arenite; Tables 1, 2; Figs. 3, 4c), the diagenetic history of this interval is relatively complex as there are several identified diagenetic processes and products based on microscopic petrography, XRD (bulk and clay), XRF and SEM analyses (Figs. 6, 7; Table 2). Based on textural relationships and relative timing of the occurrence

**Table 1** Modal analysis of the studied sandstone samples shows that monocrystalline quartz grains are dominant rock element (Starred numbers were selected for XRD, XRF and SEM analyses)

Depth, m	Petrofacies	Components, %										F type				Cement type			Pore type, %		
		Quartz	Feldspar	Chlorite	Zircon	Calcareous	Opaque	Others	Qm	Qp	Ortho-class	Plagioclase	Carbonaceous	Siliceous	Total cement	Interparticle	Vuggy	Total			
2923.55*	PF1	76	1	–	1	2	2	1	75	1	1	–	1	<1	2	15	–	15			
2923.72	PF1	81	1	–	1	1	2	1	80	1	1	–	<1	<1	–	12	–	12			
2924.01	PF1	76	2	–	1	1	1	76	–	1	1	2	<1	3	10	5	15				
2924.29	PF1	88	3	–	1	2	2	88	–	1	2	–	<1	<1	2	–	–	2			
2924.74	PF2	51	3	1	1	–	3	2	51	–	1	2	<1	39	–	–	–	0			
2924.92*	PF2	40	1	–	1	1	2	1	40	–	0.5	0.5	<1	50	5	–	–	5			
2925.2	PF2	86	2	2	1	–	5	1	86	–	1	1	<1	3	–	–	–	0			
2925.62	PF2	78	2	1	1	–	5	2	78	–	1	1	<1	3	6	2	–	8			
2926.01	PF2	85	2	–	–	–	4	1	85	–	1	1	<1	6	2	–	–	2			
2926.24	PF2	83	3	1	–	–	3	3	83	–	1	2	<1	6	1	–	–	1			
2926.58	PF2	84	2	1	–	–	6	3	84	–	1	1	<1	4	–	–	–	0			
2927.11*	PF2	85	3	1	–	–	4	2	85	–	1	2	<1	5	–	–	–	0			
2927.26	PF2	85	3	–	–	–	3	2	85	–	1	2	<1	7	–	–	–	0			
2927.64	PF2	81	2	–	1	–	2	1	81	–	1	1	<1	3	10	–	–	10			
2928.13	PF2	47	3	–	1	–	2	1	47	–	1	2	<1	46	–	–	–	0			
2928.33	PF2	86	5	–	–	–	3	2	86	–	2	3	<1	4	–	–	–	0			

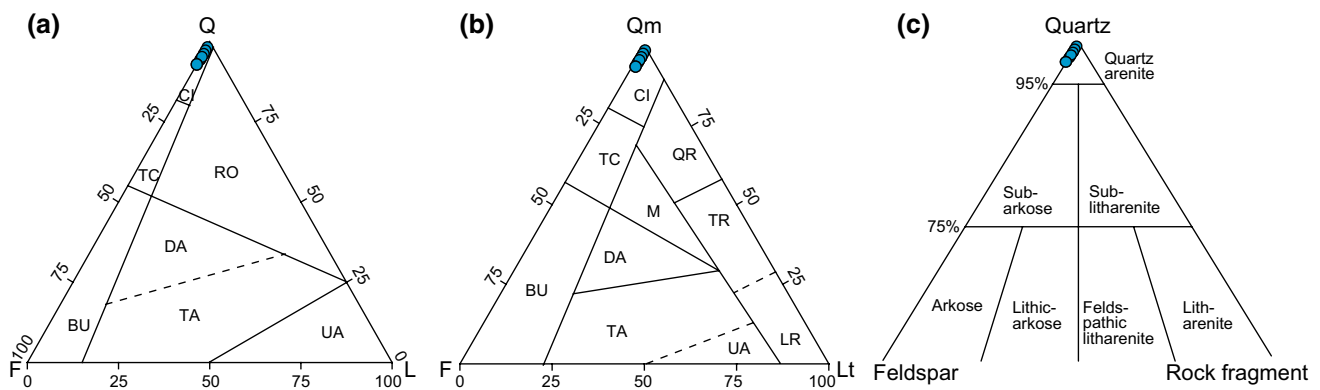


**Fig. 4** **a** Provenance determination of the Gadvan sandstone using the ternary discrimination diagrams of Dickinson and Suczek (1979) and Dickinson (1985). *Q* quartz, *F* Feldspars, *L* Lithics, *RO* Recycled Orogen, *BU* Basement Uplift, *TA* Transitional Arc, *DA* Dissected Arc, *UA* Undissected Arc, *TC* Transitional Continental, *CI* Continental Interior. **b** Provenance determination of the Gadvan sandstone using the ternary discrimination diagrams of Dickinson and Suczek (1979) and Dickinson (1985). *Qm* Quartz monocrystalline, *F* Feldspars, *Lt* Lithics, *QR* Quartzose Recycled, *TR* Transitional Recycled, *LR* Lithic Recycled. **c** Ternary plot of the studied sandstone samples shows that all samples are quartz arenite (Folk et al. 1970; Pettijohn et al. 1987)

of diagenetic processes, the recognized diagenetic features from the earliest to the latest are as follows:

**5.1.1 Physical compaction**

The evidence of physical compaction is visible as point grain to grain contacts which are changed into pressure-solution features such as concave–convex and suture contacts and finally, stylolites (Fig. 6a).

**5.1.2 Quartz overgrowth cement**

This cementation phase is not extensive and only some quartz grains are partially covered by a relatively thin layer of syntaxial quartz overgrowth (Fig. 6a, b; Table 1). Abraded and non-continuous syntaxial quartz overgrowth around the quartz grains (Fig. 6a, b) indicates a former quartz cemented clastic rock which has been recycled. So this cementation phase does not relate to the studied formation and is inherited from a former sedimentary rock or sandstone.

**5.1.3 Dissolution**

There are some partially dissolved quartz grains (pores filled by blue dyed resin; Fig. 6c–e; vuggy porosity in Table 1) that indicate a dissolution phase. Seemingly, there is a close relationship between dissolution of quartz grains and calcite cementation and replacement (Fig. 6e, f).

**5.1.4 Calcite cementation and replacement**

Calcite cement is the most dominant cement type in the studied sandstones (Tables 1, 2). It differs from replacement in quartz and plagioclase (shows ghost of calcium plagioclases’ twinning) grains and intergranular to poikilotopic types (Fig. 6f–h). However, they are related to a relatively specific cementation phase.

**5.1.5 Chlorite cementation**

Hair like chlorite crystals or plates are the main clay content of the studied samples (Fig. 6i, j). Moreover, clay mineral analysis using XRD and also XRF results show chlorite mineralogy (Fig. 7a, b; Table 2). There is a close relationship between chlorite crystals (which are visible as batches of plates; Figs. 6j, 7b) and other diagenetic features (such as calcite cements) which confirms their diagenetic nature.

**5.1.6 Dolomite (ankerite) cementation**

Ferroan-dolomite or ankerite (Fig. 7b; Table 2) is another carbonate cement phase which is basically nucleated on previously precipitated calcite cements (Fig. 6k). However, SEM micro-images show their tiny rhombs that are grown in cavities on the surface of quartz grains (Fig. 6l). These cavities are possibly due to the corrosive effect of dolomitizing or carbonaceous fluids on quartz grains (see next section). Moreover, XRD results of shales show some dolomite content (Fig. 7c).

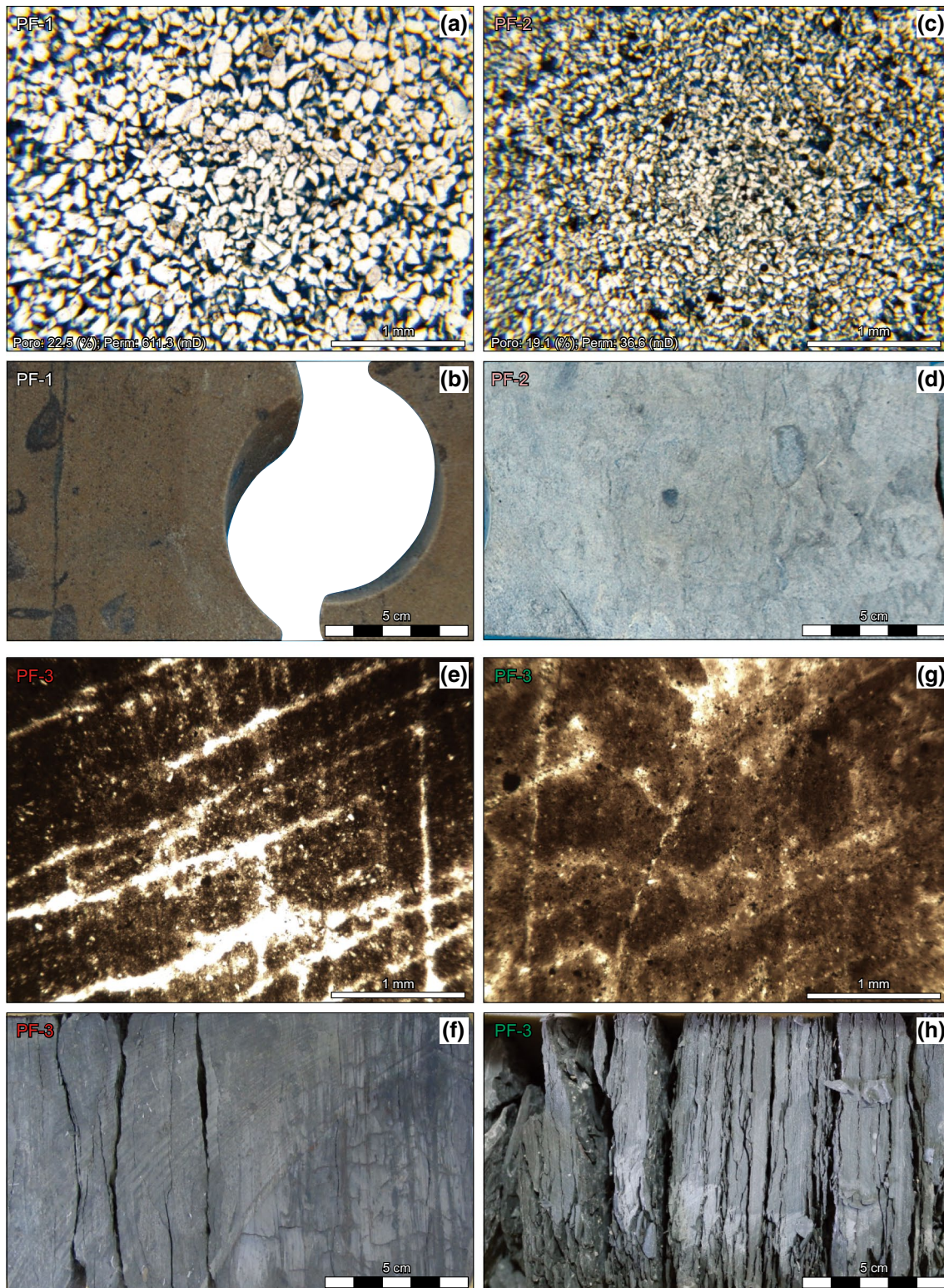


**Fig. 5** Thin section and slab photos of defined petrofacies of the Gadvan Formation. **a, b** Well sorted fine quartz arenite (PF1); **c, d** well sorted very fine quartz arenite (PF2); **e, f** silty and non-fissile shale (PF3); **g, h** fissile shale



**Table 2** The results of XRF, XRD (clay and bulk) and SEM analyses of some selected samples from the Gadvan Formation

Analysis	Depth, m	2922	2923.55	2924.92	2927.11
XRF	SiO <sub>2</sub> , %	–	90.89	70.01	–
	Al <sub>2</sub> O <sub>3</sub> , %	–	0.59	1.79	–
	Fe <sub>2</sub> O <sub>3</sub> , %	–	6.26	4.62	–
	CaO, %	–	0.44	8.07	–
	Na <sub>2</sub> O, %	–	0.08	0.16	–
	K <sub>2</sub> O, %	–	0.05	0.1	–
	MgO, %	–	0.02	2.58	–
	TiO <sub>2</sub> , %	–	0.157	0.293	–
	MnO, %	–	0.048	0.236	–
	P <sub>2</sub> O <sub>5</sub> , %	–	0.012	0.026	–
	S, %	–	0.132	0.382	–
XRD	L.O.I, %	–	1.09	11.85	–
	Cl, ppm	–	952	1096	–
XRD	Bulk	Al <sub>2</sub> Si <sub>2</sub> O <sub>5</sub> ; SiO <sub>2</sub> ; CaCO <sub>3</sub> ; CaMg(CO <sub>3</sub> ) <sub>2</sub> ; FeS <sub>2</sub> ; KAl <sub>2</sub> Si <sub>3</sub> AlO <sub>10</sub> (OH) <sub>2</sub>	SiO <sub>2</sub>	SiO <sub>2</sub> ; Ca(Fe, Mg)(CO <sub>3</sub> ) <sub>2</sub>	–
	Clay	Kaolinite; Illite	Chlorite	Chlorite	–
SEM	Dominant mineralogy	Kaolinite	Quartz	Quartz; Dolomite; Clay	Quartz; Dolomite

### 5.1.7 Pyritization

Dispersed pyrite single crystals or patches cover most of the diagenetic features such as carbonate cements (Figs. 6m, 7c; Table 1). They are recognizable in all studied samples (both sandstone and shale).

### 5.1.8 Chemical compaction

In the studied sandstones the chemical compaction features include tangential, long, concave–convex and suture grain to grain contacts (Fig. 6a, n) which finally changed into stylolites and solution seams (Fig. 6o, p) as an effect of progressive compaction. However, stylolites and solution seams are more evident in sandstone and shale, respectively.

### 5.1.9 Bitumen staining

In general, all stylolites and solution seams are stained with bitumen (or dead oil) which sometimes extended toward adjacent intergranular pores (Fig. 6p, q).

### 5.1.10 Stylolite-related dolomitization

In some parts of the studied sandstone, there are some concentrations of dolomite rhombs around the stylolites and solution seams which are termed stylolite-related dolomites (Fig. 6r, s) that geochemical data show ferroan-dolomite or ankerite (Fig. 7b and Table 2).

## 5.2 Diagenetic history

Regarding all recognized diagenetic features and their relative timing and textural relationships, the reconstructed diagenetic sequence of the studied formation is shown in Fig. 8. Generally, most diagenetic features are basically related to the late diagenesis (Morad et al. 2000; Fig. 8) and only physical compaction is from early diagenesis (Fig. 8). However, based on the primary mineralogical composition of the studied quartz arenite unit (approximately pure quartz) and visited diagenetic features, most of diagenetic minerals are allogenic and related to a possible external source. Based on the available analyses, the most probable source in the studied sandy tongue of the Gadvan Formation is its surrounding argillaceous sediments (Gadvan shales and marls; Fig. 2). Burial diagenesis of these argillaceous sediments (such as clay transformation) could lead to many secondary mineralogical phases (Table 1).

## 6 Reservoir classification

In order to evaluate reservoir properties of the studied sandy interval and defined depositional facies, several geological parameters such as facies, diagenesis, visually estimated porosity and pore types were integrated with core poro-perm data (Figs. 9, 10). The poro-perm cross-plot shows that there is a wide range of poro-perm values (porosity: 9%–23%; permeability: 0.6–1221 mD; mainly porosity > 15% and permeability > 10 mD) with a fair correlation coefficient (0.655;

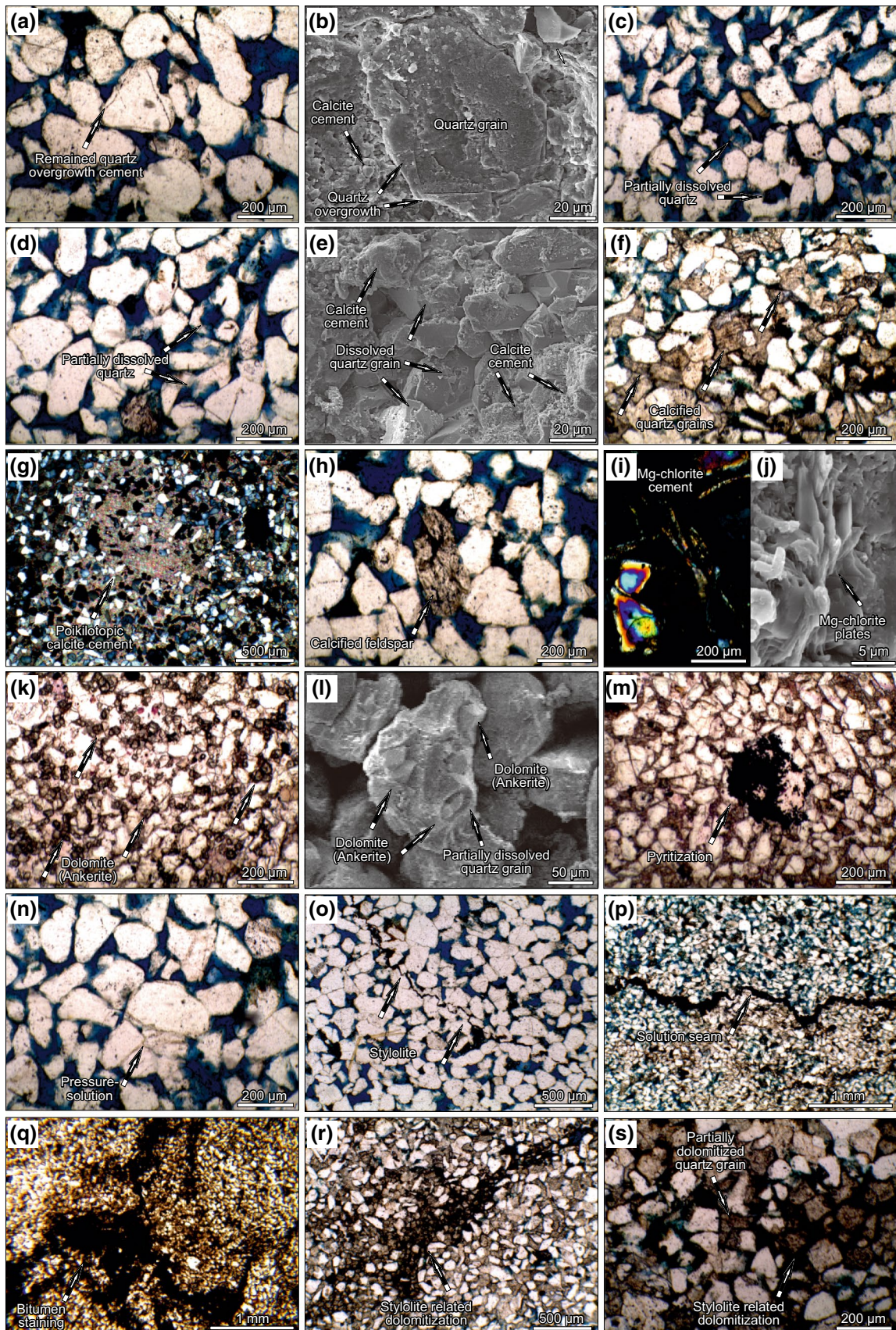


**Fig. 6** Main diagenetic features in the lower Cretaceous Gadvan sandstones. **a** Abraded Quartz overgrowth; **b** SEM photomicrograph of quartz overgrowth; **c, d** partially dissolved quartz grains; **e** SEM image of calcite cement, partially dissolved quartz grains (due to carbonate cementation); **f** calcified quartz grains; **g** poikilotopic calcite cement; **h** calcified calcium Plg; **i** chlorite cement; **j** SEM image of chlorite cement; **k** fine Fe-dolomite (ankerite) rhombs; **l** SEM photomicrograph of grown ankerite on quartz grain's surface; **m** pyritization; **n** pressure—solution and sutured contacts of quartz grains; **o** stylolitization; **p** solution seam; **q** bitumen staining; **r, s** stylolite-related dolomitization

Fig. 9a). The poroperm cross-plot of the identified petrofacies indicates that the highest poroperm values are related to PF1, and PF2 has lower and widely varying poroperm values (Fig. 9b).

A combination of all depo-diagenetic and petrophysical properties led to three main rock types each of which has a unique poroperm value and depo-diagenetic characteristics as follow (Figs. 9b, c, 10).

### 1. Rock type-1

This rock type has the highest reservoir potential and poroperm values (mean porosity: 21.7% and mean permeability: 893.2 mD) and located in the uppermost part of the studied interval (Figs. 9b, 10). It is wholly composed of PF1 and shows the lowest diagenetic modification such as low chemical compaction, weak quartz dissolution (rare vugs) and very low cementation (only rare quartz overgrowths) and quartz dissolution (Figs. 9c, 10). The very good reservoir quality of this rock type is related to its depositional characteristics including grain size (fine sand and larger pore size vs. very fine sand and smaller pores) and weak development of reservoir quality decreasing diagenetic processes (Figs. 9c, 10).

### 2. Rock type-2

This rock type is composed of PF2 and shows fair reservoir quality (mean porosity: 18.5% and mean permeability: 50.5 mD) and concentrated in the middle part of the studied interval (Figs. 9b, 10). Chemical compaction (stylolite development) and bitumen staining are the main diagenetic processes and siliceous and carbonate cementations are minor. High development of stylolites and finer grain size led to lower poroperm values in comparison with Rock type-1 (Figs. 9c, 10). So, both depositional and diagenetic features decreased the reservoir quality of this rock type.

### 3. Rock type-3

This rock type is composed of PF2 like Rock type-2 but shows low reservoir quality (mean porosity: 13.5%

and mean permeability: 2.4 mD; Figs. 9b, 10) and distributed in several parts of the studied interval (Fig. 10). In comparison with other rock types this type shows very low permeability but fair porosity which could be due to micro-porosity. The main diagenetic characteristics of this rock type are high carbonate cementation and replacement, and/or chemical compaction (Figs. 9c, 10) and shows highest diagenetic modification among the defined rock types (Fig. 9b, c).

## 7 Discussion

The succession of all diagenetic processes can be subdivided into two main stages which are illustrated in Fig. 11. The diagenetic processes of Stage-1 are physical compaction, quartz dissolution, calcite cementation and replacement, and chlorite cementation. Dolomite (ankerite) cementation, pyritization, chemical compaction, bitumen staining, and stylolite-related dolomitization are the Stage-2 diagenetic processes (Fig. 11). There is a close relationship between all diagenetic processes that took place in each stage.

### 1. Stage-1

After physical compaction (point contacts between quartz grains), dissolution of quartz grains, calcite cementation and replacement (in quartz and feldspar; Fig. 6c–h), and chlorite cementation (Fig. 6i, j) took place contemporaneously which could be related to a series of reactions which release  $H^+$  and  $Ca^{2+}$  ions and  $CO_2$  (Fig. 11). Seemingly, calcite cementation (and replacement) and quartz dissolution have been bypassing processes to prevent the collapse of the remnant quartz grains after partial dissolution (Brenner et al. 1991). The dissolution of quartz grains and precipitation of carbonate (calcite) cement could be induced by high concentration of  $Ca^{2+}$  and  $H_2CO_3$  in pore water (Fig. 8; Pettijohn et al. 1987), and increasing temperature during burial (higher solubility of quartz grains; Robinson et al. 1985) which is favorable for  $CaCO_3$  precipitation (Siever 1959). Moreover, thermal degradation of short chain carboxylic acids in organic sediments of prodelta facies (Ali and Nasser 1989; upper and lower argillaceous intervals; Fig. 2) is another source for  $CaCO_3$  cementation (Surdam et al. 1989) via dissolution of carbonate grains (Fig. 3; Table 1), movement of  $H^+$ , dissolved  $Ca^{2+}$ , and  $CO_2$  to the neighboring sandstones (Fig. 11; Miliken and Land 1991).

However, there are some partially dissolved and non-cemented quartz grains which indicate incomplete carbonate cementation and replacement (Fig. 6c, d). Based on the chemical equation in Fig. 11, with proceeding burial, the reaction of clay minerals such as kaolinite with dolomite and quartz grains (Figs. 7c, 5e) in the surrounding shales

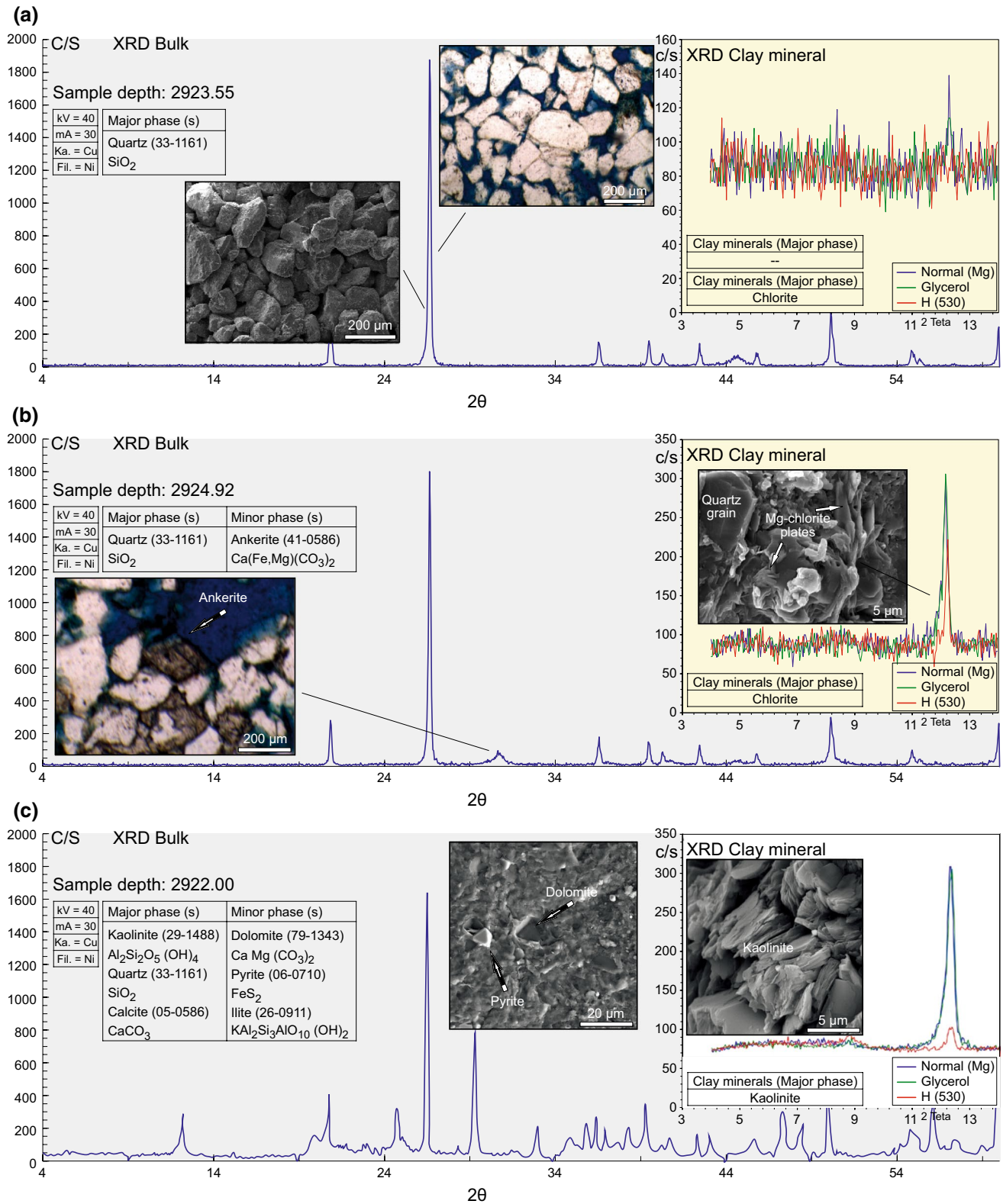


**Fig. 7** **a, b** Bulk and clay XRD analyses of PF1 and PF2 show that quartz is major mineralogical phase and chlorite is the main clay mineral. **c** Bulk and clay XRD analyses of PF3 indicate high kaolinite and quartz and calcite are major phases

Diagenetic process	Early diagenesis	Late diagenesis
Physical compaction	█	
(Quartz) dissolution		█
Calcite cementation and replacement		█
Chlorite cementation		█
Dolomite (Ankerite) cementation		█
Pyritization		█
Chemical compaction		█
Bitumen staining		█
Stylolite related dolomitization		█

**Fig. 8** Proposed diagenetic sequence of the studied interval (Morad et al. 2010; Lai et al. 2015). Only one diagenetic process is related to early diagenesis and other processes indicate late diagenesis

(Hasan 2011) can produce (Mg-) chlorite (Figs. 6i, j, 7b; Table 2) and also carbonate cements via releasing H<sup>+</sup> ions and CO<sub>2</sub> (Hutcheon et al. 1980; Bjørlykke 1988; Molenaar 1989). Moreover, generated CO<sub>2</sub> can be involved in other reactions to produce more calcite cement (Fig. 11).

2. Stage-2

The second stage and its processes (Figs. 11, 6k-s) show a deeper burial and later diagenesis phase (e.g., Taylor 1990; Morad 1998; Hendry et al. 2000; Machel 2001, 2004). High pressure solution and development of stylolites and solution seams (Fig. 6n-p) and high bitumen staining (Fig. 6q) along them, indicate the oil window and high temperature and pressure conditions (Machel 2004) which led to chemical compaction and dissolution of

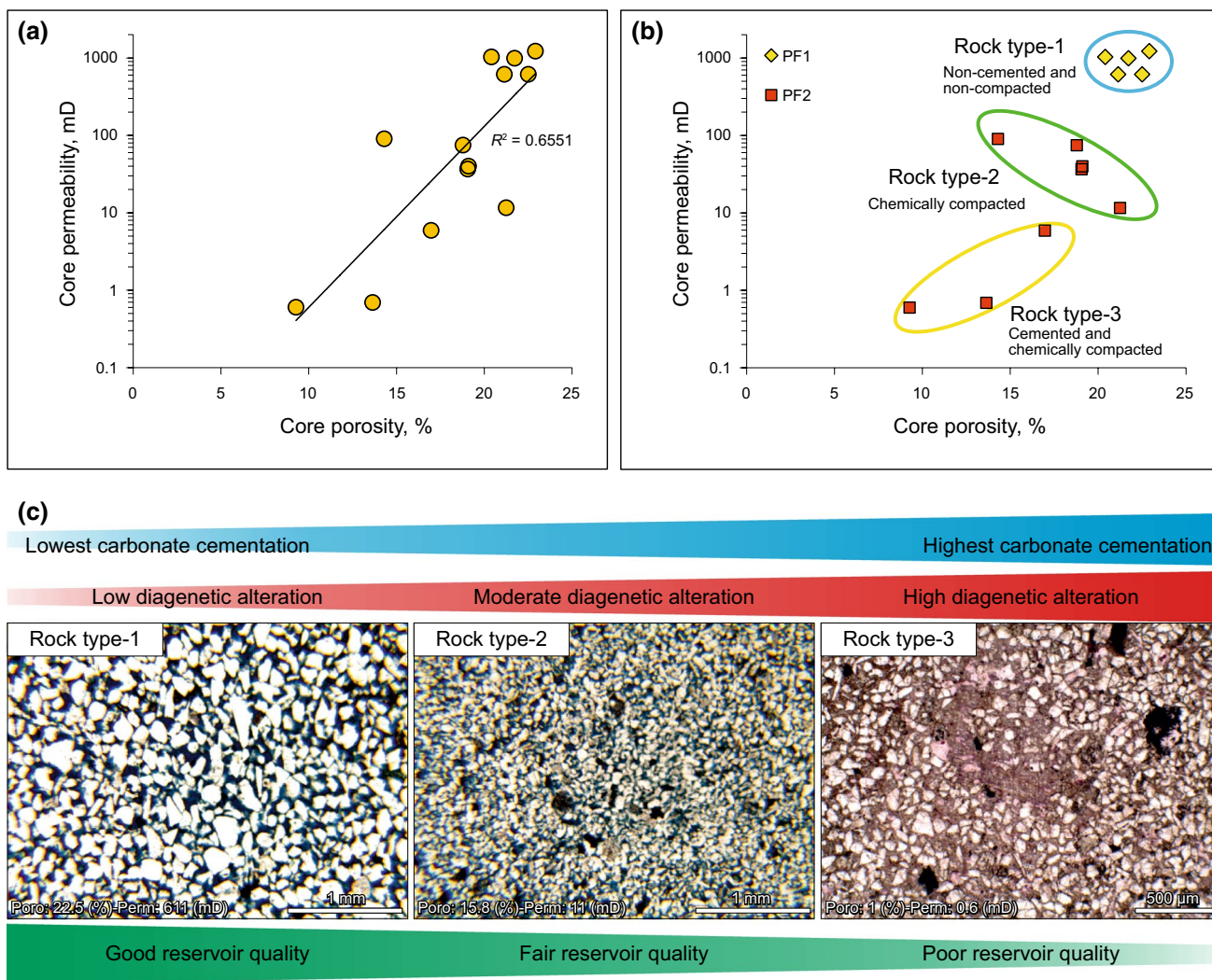
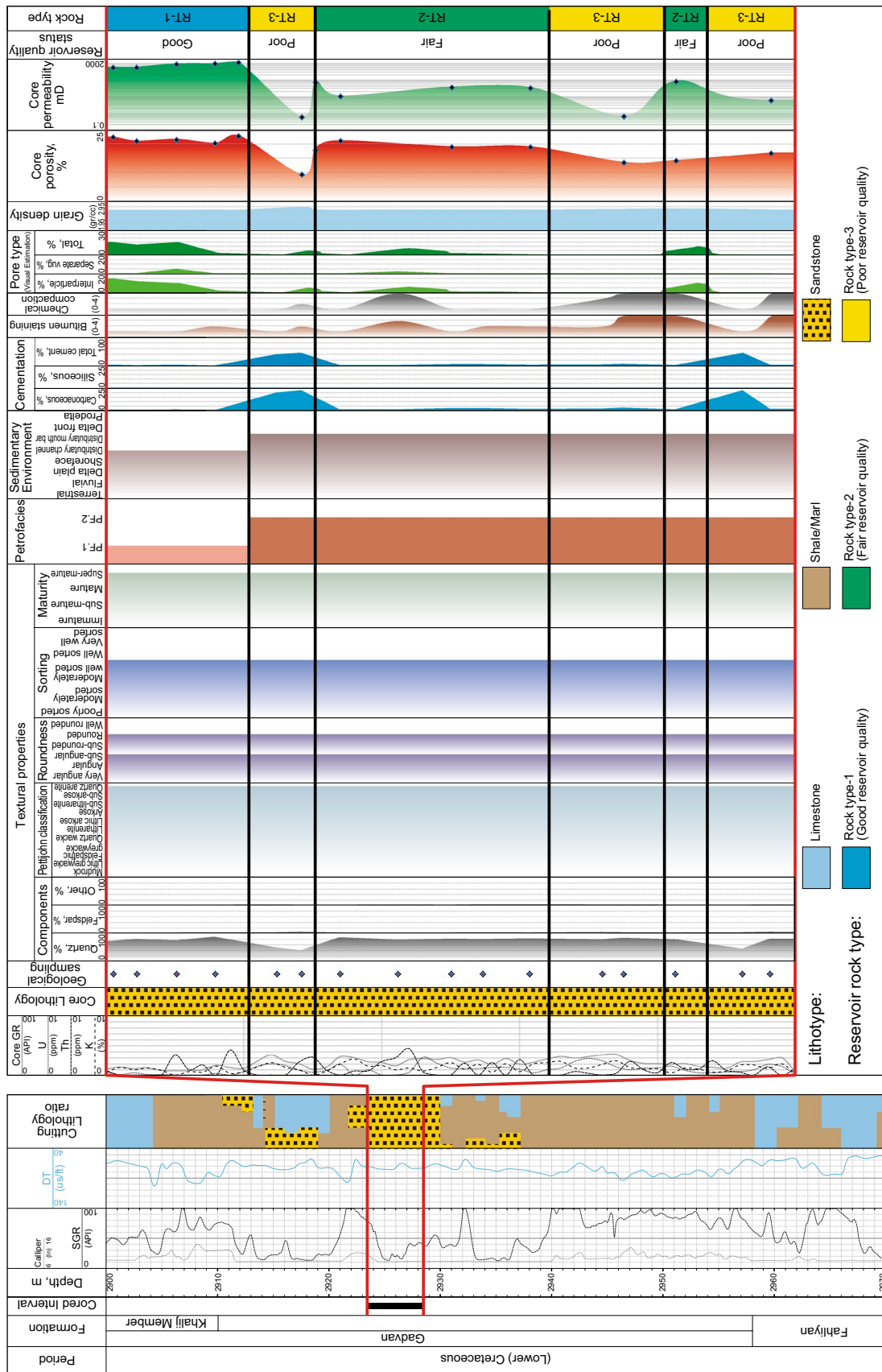


**Fig. 9** a Poroperm cross-plot of the studied samples shows a discrete pattern. b Poroperm cross-plot of the studied samples based on petrofacies types and defined rock types (zone numbers refer to Fig. 10). c Samples of three main identified rock types which are sorted based on their reservoir quality and diagenetic alteration



◀**Fig. 10** Composite depo-diagenetic and reservoir stratigraphic profile of the studied sandy interval. The reservoir zones (reservoir quality column) are defined based on poroperm values but the rock types are recognized using both depo-diagenetic and poroperm characteristics

quartz grains (Robinson et al. 1985). An  $\text{Fe}^{2+}$  source is the main parameter in formation of both ankerite and pyrite and also  $\text{S}^{2-}$  for pyrite. Regarding a rare internal source for these diagenetic phases (some dispersed phytoclasts), at least  $\text{Fe}^{2+}$  and  $\text{S}^{2-}$  ions are related to the neighboring argillaceous rocks as bitumen staining along the stylolites and seams. Petrographic evidence shows that the main carbonate source of ankerite cements has been former calcite cements (as replacement in calcite crystals) and some of them have been grown as quartz replacement (Fig. 6k, l). Under thermobaric regimes, clays (mixed layer and illite; Fig. 7c) conversion and thermal degradation of organic matter in the open marine argillaceous intervals can provide needed  $\text{Mg}^{2+}$  and  $\text{Fe}^{2+}$  for ankerite generation (Taylor 1990; Brenner et al. 1991). Also, introduction of  $\text{H}_2\text{S}$  into the pore water before peak migration of hydrocarbon could have provided the needed sulfur for the formation of pyrite (Robinson et al. 1985; Fig. 6m). Stylolite-related dolomitization occurred as the final diagenetic product which is visible around the stylolites in carbonate cemented zones (Fig. 6r, s).

A combination of both geological and petrophysical (poroperm) data led to the identification of rock types that are appropriate for 2D and 3D reservoir modeling (e.g., Lucia 1995; Gomes et al. 2008). In the studied interval, the reservoir quality of each rock type is affected by different proportions of depositional and diagenetic processes. From Rock type-1 to Rock type-3 in a descending order of reservoir potential, the proportion of diagenetic alteration (mainly carbonate cementation) is increased (Fig. 10). Investigations show that the very good reservoir quality of Rock type-1 is only related to depositional characteristics (high interparticle porosity) (Figs. 9c, 10). Also, the low reservoir quality of Rock type-3 is basically controlled by diagenetic alteration (high carbonate cementation and replacement) as a probable result of expelling burial fluids from the burial diagenesis of the surrounding mudrocks

(Figs. 8, 9c, 10). The fair reservoir quality of Rock type-2 is related to both depositional and diagenetic properties which are chemical compaction and remained interparticle porosity (Figs. 9c, 10).

In general, the studied interval is composed of a thick package of PF2 facies (very fine quartz arenite), which due to heterogeneous carbonate cementation it is composed of two upper and lower cemented units that resulted in alternative reservoir and non-reservoir units (Rock type-2 and Rock type-3; Fig. 10).

## 8 Conclusions

1. The studied sandy part of the lower Cretaceous Gadvan Formation in SW Iran is mainly composed of quartz arenite and also two petrofacies which are related to distributary channels and mouth bars that are embedded in prodelta and open marine shales and marls.
2. The ternary discrimination diagrams for provenance of sandstones of the studied clastic interval indicate a continental interior depositional setting.
3. This relatively depositionally homogenous siliciclastic unit has been affected by several (late) diagenetic processes. Most of diagenetic features (basically carbonate cementation) are related to the burial diagenesis of the surrounding argillaceous successions and expelling burial fluids.
4. The succession of diagenetic processes is subdivided into two main stages. Stage-1 processes are physical compaction, quartz overgrowth, quartz dissolution, calcite cementation and replacement, and chlorite cementation., Stage-2 diagenetic processes are dolomite (ankerite) cementation, pyritization, chemical compaction, bitumen staining, and stylolite-related dolomitization
5. The main diagenetic features of this sandy unit are carbonate (calcite and dolomite) cementation and replacement, and chlorite cementation which their constituents (such as  $\text{H}^+$ ,  $\text{Ca}^{2+}$ ,  $\text{Mg}^{2+}$ ,  $\text{Fe}^{2+}$ ,  $\text{S}^{2-}$  and  $\text{CO}_2$ ) have originated from clay conversion and thermal degradation and maturation of organic matter in the adjacent argillaceous intervals.
6. An integration of depositional, diagenetic and petrophysical characteristics revealed that this primarily porous, homogenous and clean sandstone reservoir has been changed into a heterogeneous (alternative reservoir and non-reservoir units) and cemented reservoir rock under the burial condition and during late diagenesis of the adjacent mudrocks.

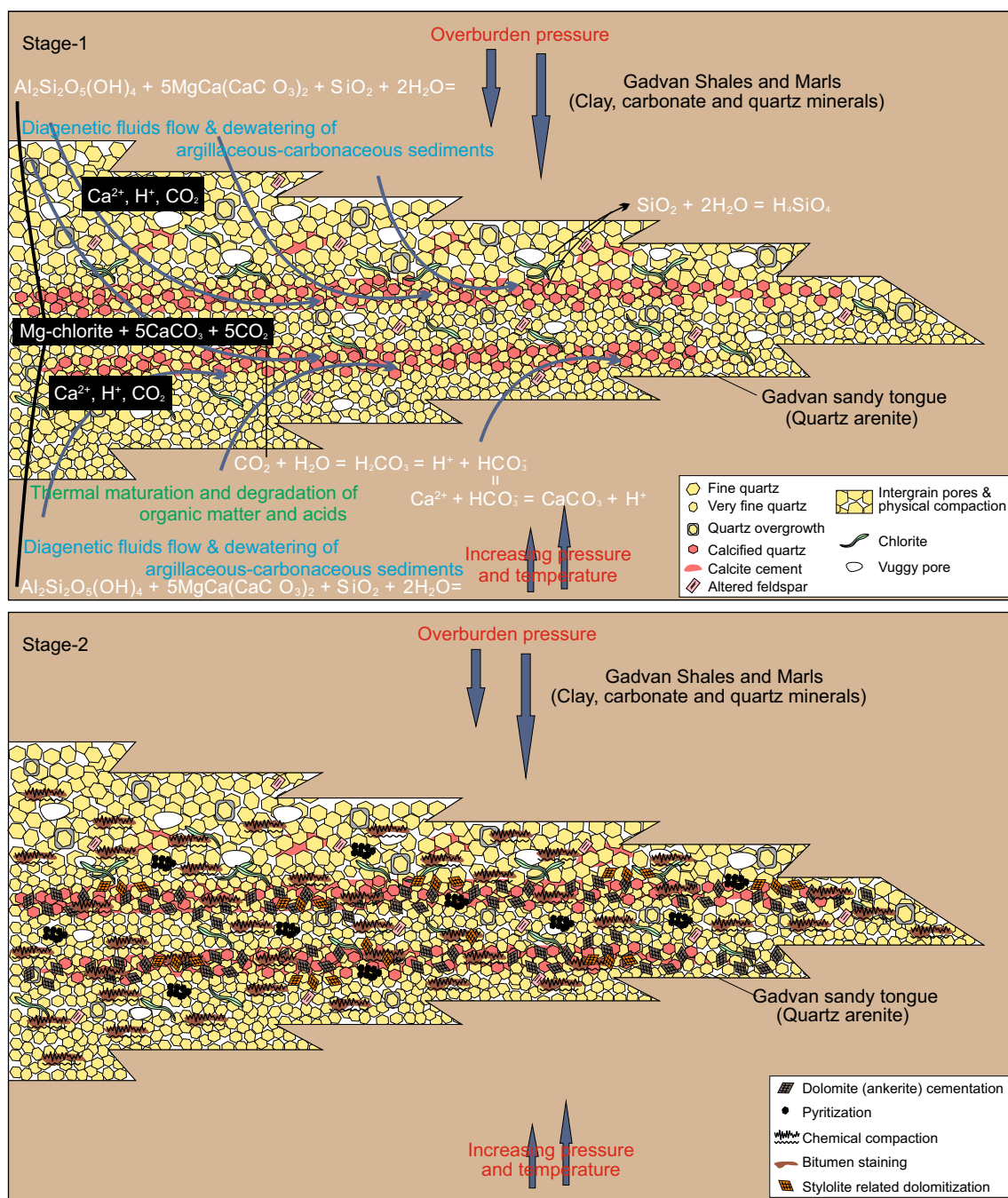


**Fig. 11** A schematic diagenetic history of the studied sandstone interval. In general, all diagenetic features are related to two main stages. During the first stage a series of processes such as calcite replacement and cementation, feldspar alteration, and dissolution have taken place. Then, ankerite cementation, chemical compaction, stylolite-related dolomitization, bitumen staining, and pyritization are final diagenetic features

**Acknowledgements** The NIOC is thanked for data preparation and sponsorship. Special thanks go to H. Mehrabi for his review and invaluable comments. Three other anonymous reviewers are thanked for their helpful comments and reviews. We would like to acknowledge the Editorial staff of the Journal of Petroleum Science.

**Open Access** This article is distributed under the terms of the Creative Commons Attribution 4.0 International License (<http://creativecommons.org/licenses/by/4.0/>), which permits unrestricted use, distribution, and reproduction in any medium, provided you give appropriate credit to the original author(s) and the source, provide a link to the Creative Commons license, and indicate if changes were made.



## References

- Ahr WM. Geology of carbonate reservoirs. London: Wiley; 2008. p. 277. <https://doi.org/10.1002/9780470370650>.
- Al-Ameri TK, Batten DJ. Palynomorph and palynofacies indications of age, depositional environments and source potential for hydrocarbons: lower Cretaceous Zubair Formation, southern Iraq. *Cretaceous Res.* 1997;18:789–97. <https://doi.org/10.1006/cres.1997.0087>.
- Al-Fares AA, Bouman M, Jeans P. A new look at the Middle to Lower Cretaceous stratigraphy offshore Kuwait. *Geo Arabia.* 1998;3(4):543–60. <https://eurekamag.com/research/029/703/029703797>.
- Ali AJ, Nasser ME. Facies analysis of the lower Cretaceous oil-bearing Zubair Formation in southern Iraq. *Mod Geol.* 1989;13:225–42. <https://eurekamag.com/research/018/908/018908121.php>.
- Al-Rawi MM. Geological interpretation of oil entrapment in the Zubair formation Raudhatain Field. In: Society of petroleum engineers Middle East oil technical conference Bahrain, vol. 9591. SPE; 1981. p. 149–59. <https://doi.org/10.2118/9591-MS>.
- Alsharhan AS, Nairn AEM. Carbonate platform models of Arabian Cretaceous reservoirs. In: Simo JAT, Scott RW, Masse JP, editors. *Cretaceous carbonate platforms*. AAPG Memoir, vol. 56. 1993. p. 148–73. <https://doi.org/10.1306/M56578>.
- Alsharhan AS, Nairn AEM. *Sedimentary basins and petroleum geology of the Middle East*. 2nd ed. Amsterdam: Elsevier; 2003. p. 843. <https://doi.org/10.1016/B978-0-444-82465-3.X5000-1>.
- Agrawi AAM, Goff JC, Horbury AD, Sadooni FN. The petroleum geology of Iraq. Beaconsfield: Scientific Press Ltd; 2010. p. 424. <https://doi.org/10.1111/j.1747-5457.2010.00487.x>.
- Bayet-Goll A, Samani PN, de Carvalho CN, et al. Sequence stratigraphy and ichnology of Early Cretaceous reservoirs, Gadvan Formation in southwestern Iran. *Mar Pet Geol.* 2016;81:294–319. <https://doi.org/10.1016/j.marpetgeo.2016.11.008>.
- Bjørlykke K. Sandstone diagenesis in relation to preservation, destruction, and creation of porosity. In: Chilingarian CV, Wolf KH, editors. *Diagenesis: developments in sedimentology*, vol. 41. Amsterdam: Elsevier; 1988. p. 555–588. [https://doi.org/10.1016/S0070-4571\(08\)70180-8](https://doi.org/10.1016/S0070-4571(08)70180-8).
- Brenner RL, Ludvigson GA, Scal R, Dogan AU. Diagenetic modeling of siliciclastic systems; status report. *Bull Kans State Geol Surv.* 1991;233:123–37. <http://www.kgs.ku.edu/Publications/Bulletins/233/Brenner/index.html>.
- Buday T. The regional geology of Iraq. Volume I: stratigraphy and palaeogeography. Baghdad: Publications of GEOSURV; 1980. p. 445. <https://books.google.com/books?id=wVxPAQAIAAJ>.
- Burrows A, Moss A, Sirju C, Pritchard T. Improved permeability prediction in heterogeneous carbonate formations. In: SPE. 2010. p. 131606. <https://onepetro.org/conference-paper/SPWLA-2015-GGG>
- Dana JD. *Manual of mineralogy*. London: Wiley; 1985. p. 596.
- Dickinson WR. Interpreting provenance relations from detrital modes of sandstones. In: Zuffa GG, editor. *Provenance of arenites*. Dordrecht. The Netherlands, Reidel Publishing Company, NATO Advanced Study Institute, vol. 148. 1985. p. 333–61. <https://doi.org/10.1007/978-94-017-2809-6>.
- Dickinson WR, Suzek CA. Plate tectonics and sandstone composition. *AAPG Bull.* 1979;63:2164–82. <https://doi.org/10.1306/2F9188FB-16CE-11D7-8645000102C1865D>.
- Ebanks Jr WJ, Scheihing MH, Atkinson CD. Flow units for reservoir characterization. In: Morton-Thompson D, Woods AM, editors. *Development geology reference manual*. AAPG, Methods in Exploration Series, vol. 10. 1992. p. 541. <https://doi.org/10.1306/Mth10573>.
- Enayati-Bidgoli AH, Rahimpour-Bonab H. A geological based reservoir zonation scheme in a sequence stratigraphic framework: a case study from the Permo-Triassic gas reservoirs, Offshore Iran. *Mar Pet Geol.* 2016;73:36–58. <https://doi.org/10.1016/j.marpetgeo.2016.02.016>.
- Folk RL. Stages of textural maturity in sedimentary rocks. *J Sediment Pet.* 1951;21:127–30. <https://doi.org/10.2110/jsr.21.127>.
- Folk RL. Bimodal supermature sandstones. Product of the desert floor. In: XXIII international geological congress proceedings, vol. 8. 1968. p. 9–32.
- Folk RL, Andrews PB, Lewis DW. Detrital sedimentary rock classification and nomenclature for use in New Zealand. *J Geol Geophys.* 1970;13:937–68. <https://doi.org/10.1080/00288306.1970.10418211>.
- Ghazban F. *Petroleum geology of the Persian Gulf*. Tehran University and National Iranian Oil Company. 2007. p. 707.
- Gomes JS, Riberio MT, Strohmenger CJ, et al. Carbonate reservoir rock typing—the link between geology and SCAL. In: SPE. 2008. p. 118284. <https://doi.org/10.2118/118284-MS>.
- Gribble CD, Hall AJ. *Optical mineralogy*. London: UCL Press; 1995. p. 303. <https://doi.org/10.1017/S0016756800020677>.
- Haq BU, Hardenbol J, Vail PR. Mesozoic and Cenozoic chronostratigraphy and cycles of sea-level change. In: Wilgus CK, Hastings BS, Ross CA, et al., editors. *Sea level changes—an integrated approach*, vol. 42. SEPM Sp Pub. 1988. p. 407. <https://doi.org/10.2110/pec.88.01.0071>.
- Hasan IS. A sedimentological study of the Zubair Formation in the Luhais oil field Southern Iraq. Unpublished M.Sc. Thesis, Department of Geology, College of Science, University of Baghdad, Baghdad, Iraq. 2011. p. 90.
- Hendry JP, Wilkinson M, Fallick AE, et al. Ankerite cementation in deeply buried Jurassic sandstone reservoirs of the Central North Sea. *J Sediment Res.* 2000;70(1):227–39. <https://doi.org/10.1306/2DC4090D-0E47-11D7-8643000102C1865D>
- Hollis C. Diagenetic controls on reservoir properties of carbonate successions within the Albiano-Turonian of the Arabian Plate. *Pet Geosci.* 2011;17:223–41. <https://doi.org/10.1144/1354-079310-032>.
- Hutcheon I, Oldershaw A, Ghent ED. Diagenesis of Cretaceous sandstones of the Kootenay Formation at Elk Valley (southeastern British Columbia) and Mt. Allen (southwestern Alberta). *Geochim Cosmochim Acta.* 1980;44:1425–35. [https://doi.org/10.1016/0016-7037\(80\)90108-8](https://doi.org/10.1016/0016-7037(80)90108-8).
- James GA, Wynd JG. Stratigraphic nomenclature of Iranian oil consortium agreement area. *AAPG Bull.* 1965;49:2182–245.
- Jassim SJ, Goff JC, Dolin SRO. *Geology of Iraq*. Brno: Dolin Prague and Moravian Museum; 2006. p. 341. <https://books.google.com/books?id=LLH8aygMJFwC>.
- Jerram DA. Visual comparators for degree of grain-size sorting in two and three dimensions. *Comput Geosci.* 2001;27:485–92. [https://doi.org/10.1016/S0098-3004\(00\)00077-7](https://doi.org/10.1016/S0098-3004(00)00077-7).
- Lai J, Wang GW, Ran Y, et al. Predictive distribution of high-quality reservoirs of tight gas sandstones by linking diagenesis to depositional facies: evidence from Xu-2 sandstones in the Penglai area of the central Sichuan basin, China. *J Nat Gas Sci Eng.* 2015;23:97–111. <https://doi.org/10.1016/j.jngse.2015.01.026>.
- Lucia FJ. Rock-fabric/petrophysical classification of carbonate pore space for reservoir characterization. *AAPG Bull.* 1995;79(9):1275–300. <https://doi.org/10.1306/7834D4A4-1721-11D7-8645000102C1865D>.
- Lucia FJ. *Carbonate reservoir characterization*. Berlin: Springer; 2007. p. 341. <https://doi.org/10.1007/978-3-540-72742-2>.
- Machel HG. Bacterial and thermochemical sulfate reduction in diagenetic settings; old and new insights. In: Rouchy JM, Taberner C, Peryt TM, editors. *Sedimentary and diagenetic transitions between carbonates and evaporites*. *Sediment Geol.*, vol. 140.

2001. p. 143–75. [https://doi.org/10.1016/S0037-0738\(00\)00169-X](https://doi.org/10.1016/S0037-0738(00)00169-X).
- Machel HM. Concepts and models of dolomitization: a critical reappraisal. In: Braithwaite CJR, Rizzi G, Darke G, editors. The geometry and petrogenesis of dolomite hydrocarbon reservoirs, vol. 235. London: Geological Society, Special Publications; 2004. p. 7–63. <https://doi.org/10.1144/GSL.SP.2004.235.01.01>.
- McBride EF. A classification of common sandstones. *J Sediment Pet.* 1963;33:664–9. <https://doi.org/10.1306/74D70EE8-2B21-11D7-8648000102C1865D>.
- Milliken KL, Land LS. Reverse weathering, the carbonate-feldspar system, and porosity evolution during burial of sandstones (abs.). *AAPG Bull.* 1991;75:636.
- Molenaar N. Eogenetic and telogenetic cementation of sandstones. *Geol Ultraiect.* 1989;58:126.
- Moore CH. Carbonate reservoirs porosity evolution and diagenesis in a sequence stratigraphic framework. Amsterdam: Elsevier; 2001. p. 444. [https://doi.org/10.1016/S0146-6380\(01\)00104-8](https://doi.org/10.1016/S0146-6380(01)00104-8).
- Morad S. Carbonate cementation in sandstones: distribution patterns and geochemical evolution. In: Morad S, editor. Carbonate cementation in sandstones: distribution patterns and geochemical evolution. Oxford: Blackwell Publishing Ltd.; 1998. p. 528. <https://doi.org/10.1002/9781444304893.ch1>.
- Morad S, Ketzer JM, De Ros LF. Spatial and temporal distribution of diagenetic alterations in siliciclastic rocks: implications for mass transfer in sedimentary basins. *Sedimentology.* 2000;47:95–120. <https://doi.org/10.1046/j.1365-3091.2000.00007.x>.
- Morad S, Al-Ramadan K, Ketzer JM. The impact of diagenesis on the heterogeneity of sandstone reservoirs: a review of the role of depositional facies and sequence stratigraphy. *AAPG Bull.* 2010;94:1267–309. <https://doi.org/10.1306/04211009178>.
- Morad S, Ketzer JK, De Ros LF. Linking diagenesis to sequence stratigraphy. *Int Assoc Sediment.* 2012;45:536. <https://doi.org/10.1002/9781118485347>
- Pettijohn FJ, Potter PE, Siever R. Sand and sandstone. 2nd ed. New York: Springer; 1987. p. 553. <https://doi.org/10.1007/978-1-4612-1066-5>.
- Powers MC. A new roundness scale for sedimentary particles. *J Sediment Pet.* 1953;23:117–9. <https://doi.org/10.1306/D4269567-2B26-11D7-8648000102C1865D>.
- Powers RW, Ramirez LF, Redmond CD, et al. Geology of the Arabian Peninsula: sedimentary geology of Saudi Arabia. United States Geological Survey Professional Paper, vol. 560-D. 1966. p. 147. <https://doi.org/10.3133/pp560D>.
- Robinson RJ, Chaudhuri S, Jones LM. Diagenesis of the Pennsylvanian Morrowan sandstone, Clark County, Kansas. *Sub Geol Ser.* 1985;6:56–65. <http://www.kgs.ku.edu/Publications/Bulletins/Sub6/Robinson/index.html>.
- Sadooni F, Aqrabi AAM. Cretaceous sequence stratigraphy and petroleum potential of the Mesopotamian Basin, Iraq. In: Alsharhan A, Scott B, editors. Middle East models of Jurassic Cretaceous carbonate systems, vol. 69. SEPM Spec Pub.; 2000. p. 315–34. <https://doi.org/10.2110/pec.00.69>.
- Scott RW, Simo JA, Masse J-P. Overview of economic resources in Cretaceous carbonate platforms. In: Simo JA, Scott RW, Asse JP, editors. Cretaceous Carbonate Platforms. AAPG Mem., vol. 56. 1993. p. 15–24. <https://doi.org/10.1306/M56578>.
- Setudehnia A. The Mesozoic sequence in southwest Iran and adjacent areas. *J Pet Geol.* 1978;1:3–42. <https://doi.org/10.1111/j.1747-5457.1978.tb00599.x>.
- Sharland PR, Archer R, Casey DM, et al. Arabian plate sequence stratigraphy. *GeoArabia Sp Pub.* 2001;2:371.
- Siever R. Petrology and geochemistry of silica cementation in some Pennsylvanian sandstones. In: Silica in sediments—a symposium, vol. 7. SEPM Sp Pub.; 1959. p. 55–79. <https://doi.org/10.2110/pec.59.01.0055>.
- Slatt RM. Stratigraphic reservoir characterization for petroleum geologists and engineers. 1st ed. Amsterdam: Elsevier; 2006. p. 47.
- Slatt RM, Galloway WE. Geological Heterogeneities. In: Morton-Thompson D, Woods AM, editors. Development geology reference manual. AAPG, Methods in Exploration Series, vol. 10. 1992. p. 541. <https://doi.org/10.1306/Mth10573>.
- Surdam RC, Crossey LJ, Hagan ES, et al. Organic–inorganic interactions and sandstone diagenesis. *AAPG Bull.* 1989;73:1–23. <https://doi.org/10.1306/703C9AD7-1707-11D7-8645000102C1865D>.
- Taylor TS. The influence of calcite dissolution on reservoir porosity in Miocene sandstones, Picaroon Field, offshore Texas Gulf Coast. *J Sediment Res.* 1990;60:322–34. <https://doi.org/10.1306/212F9192-2B24-11D7-8648000102C1865D>.
- Wentworth CK. A scale of grade and class terms for clastic sediments. *J Geol.* 1922;30:377–92. <https://www.jstor.org/stable/30063207>
- Zeigler MA. Late permian to holocene paleofacies evolution of the arabian plate and its hydrocarbon occurrences. *GeoArabia.* 2001;6:445–504.